Green's Function Expansions in Cylindrical Waves and Its Rigorous Source Singularity Evaluation for Full-Wave Analysis of SIW Radiating Structures

Final Report

By Guido Valerio

Introduction

Substrate Integrated Waveguides (SIW), have been recently provided a class of innovative waveguide based, high frequency circuits [1]-[8] (see Fig. 1 (a)). They can be realized using standard printed circuit board (PCB) technology, of low cost and easy production. Waveguide channels are realized on a grounded dielectric slab by using arrays of metallic vias. SIW technology maintains the advantage of metallic waveguides in addition with the possibility of integration typical of microstrip structures, allowing sophisticated packaging technology and the integration of complex beam-forming networks and antennas on the same boards. The radiating parts of these devices can be practically implemented through slotted arrays present on the top metallic plate (see Fig. 1 (b)).

Different approaches have been proposed to perform analyses of wave propagation in SIW configurations. Approximate method has been found by considering metallic waveguide equivalent to the SIW ones and resorting to the technique adopted for conventional waveguide. Alternatively, homogenized boundary conditions could be derived to replace the lateral vias with a homogeneous condition. On the other hand, despite being computationally efficient, these approaches cannot ensure the correctness of the final design results.

Unfortunately, if a rigorous solution is required, because of the presence of vias forming the lateral walls of the waveguide, a finite difference or finite element type of solution needs to be often employed. The design of real device using quasi-optical system (electrically very large structure) is then considerably time consuming and memory demanding.

A code is currently under development at IETR, capable to efficiently study large waveguide structures realized in SIW technology by means of a mode matching approach, based on cylindrical wave expansions of the fields scattered by the metallic posts. The aim of the present project consists in the treatment of the code capabilities with reference to the analyses of slotted SIW structures by means of a rigorous method-of-moment approach.

For the analysis of slotted waveguides, the computation of coupling terms between different slots present on the same ground plane is of paramount importance. The computation of electric-field dyadic Green's functions is then required for source and observation points on the same horizontal plane. To this aim, correct expressions for source singularities are required in order to accurately evaluate, for instance, self-admittance terms. We are here referring mainly to two different approaches for the derivation of field dyadic Green's functions, which can be summarized as Felsen's and Chew's derivations. While these referenced expressions are found in a general coordinate system, we are interested to the specific expression of the Green's functions in a cylindrical coordinate system, due to the geometrical symmetry of the SIW problem.

In the following sections, singularities arising on the source plane, due to the cylindrical choice of coordinate system will be investigated analytically, by resorting to the Chew formulation for the relevant Green's functions.

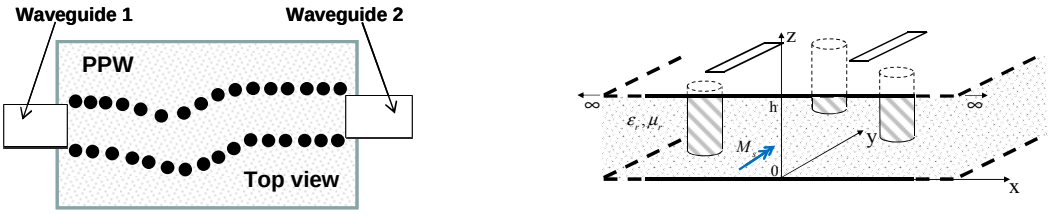

(a) (b)

Fig. 1. Typical geometry of a SIW waveguide fed by waveguides. (a) Top view, (b) lateral view, with slots on the top metallic plate.

I – Formulation of Cylindrical-Wave Dyadic Green's Functions

Assuming time-harmonic excitation of the form $\exp(+j\omega t)$, the dyadic Green's function is defined as the solution to the following partial differential equation:

$$\nabla \times \nabla \times \bar{\bar{G}}(r,r') - k_0^2 \bar{\bar{G}}(r,r') = \bar{\bar{I}}\delta(r - r'), \tag{1}$$

where $k_0^2 = \omega^2 \varepsilon \mu$ is the medium wavenumber, and the solution $\bar{\bar{G}}(r,r')$ is subject to some prescribed boundary conditions. The geometry under consideration is a circular cylinder of non-varying cross section which may or may not be stratified in the z-direction. We may solve this equation by resorting to a Hertz potential-like expansion of the Green's function in terms of cylindrical vector wave functions defined as

$$M_n(k_\rho, k_z, r) = \nabla \times (\hat{z}\psi(r)) \tag{2a}$$

$$N_n(k_\rho, k_z, r) = \frac{1}{k}\nabla \times \nabla \times (\hat{z}\psi(r)), \tag{2b}$$

$$L_n(k_\rho, k_z, r) = \nabla(\hat{z}\psi(r)), \tag{2c}$$

where $\hat{z}$ is the so-called pilot vector and $\psi(r)$ is the solution of the scalar, source-free Helmholtz equation with the boundary conditions specified at infinity. The $\psi(r)$ function in cylindrical coordinates is given by

$$\psi(r) = J_n(k_\rho \rho) e^{-jk_z z} e^{-jn\phi}. \tag{3}$$

We may express the total Green's function as a sum of a free-space and a scattered part

$$\bar{\bar{G}}(r,r') = \bar{\bar{G}}_{free}(r,r') + \bar{\bar{G}}_{Scattered}(r,r'). \tag{4}$$

The free-space part may be obtained by expanding the dyadic delta function on the right hand side of (1) in terms of (2):

$$\bar{\bar{G}}_{free}(r,r') = \frac{1}{(2\pi)^2}\sum_{n=-\infty}^{\infty}\int_{-\infty}^{\infty} dk_z \int_0^{\infty} dk_\rho\, k_\rho \left(M_n(k_\rho, k_z, r)a(k_\rho, k_z) + N_n(k_\rho, k_z, r)b(k_\rho, k_z) + L_n(k_\rho, k_z, r)c(k_\rho, k_z)\right) \tag{5}$$

with

$$a(k_\rho, k_z) = \frac{M_{-n}(-k_\rho, -k_z, r')}{(k^2 - k_0^2)k_\rho^2}, \tag{6a}$$

$$b(k_\rho, k_z) = \frac{N_{-n}(-k_\rho, -k_z, r')}{(k^2 - k_0^2)k_\rho^2}, \tag{6b}$$

$$c(k_\rho, k_z) = -\frac{L_{-n}(-k_\rho, -k_z, r')}{k_0^2 k^2}. \tag{6c}$$

The inverse transform may be performed by integrating either in k_z or k_ρ first, which, depending on the particular choice of the order of integration, corresponds to the extraction of a pillbox-shaped volume in which the source is embedded, but with different orientation, $\hat{z}$ and $\hat{\rho}$ respectively. If the k_z integration is performed first, the unbounded medium Green's function becomes

$$\bar{\bar{G}}_{free}(r, r') = -\frac{\hat{z}\hat{z}}{k_0^2}\delta(r - r') - \frac{j}{4\pi}\sum_{n=-\infty}^{\infty}\int_0^\infty dk_\rho \left(M_n(k_\rho, \pm k_{0z}, r)M_{-n}(-k_\rho, \mp k_{0z}, r')\right.$$
$$\left. + N_n(k_\rho, \pm k_{0z}, r)N_{-n}(-k_\rho, \mp k_{0z}, r')\right)\frac{1}{k_{0z}k_\rho} \tag{8}$$

The delta term comes out of the L_n term in the expansion. In more detail, this term cannot be integrated directly since it contains a part which goes as a constant in the large k_ρ limit. Therefore, it has to be extracted so that the Jordan lemma can be applied to the remainder. The extracted part then corresponds to the delta term in **(8)**, which we recognize as the depolarizing dyad.

To account for the presence of boundaries, scattered waves must be added to the free-space waves. Since the source singularities are related with the free-space part of the Green's function, these further terms will not be detailed here.

However, one must exercise caution with this particular representation since there are extra dyadic delta terms to be extracted in the source plane due to the non-convergence of the inverse transforms of fields in the source plane z=z'. The free-space part of the Green's function exhibits this behavior since the complex exponential in the inverse transform integrand behaves as a constant for all values of the transverse wave number at the source plane, as opposed to away from the source plane where it behaves oscillatory for k_ρ<k_0 and decays for k_ρ>k_0.

We perform the spectral k_z integration at the source plane term by term. We can conclude that the $\hat{\rho}\hat{z}$ and $\hat{\phi}\hat{z}$ dyads in the second and third dyadic of (5) do not contribute to the integral, since they are odd in k_z, and therefore vanishes. The integral of the first dyadic (TM_z) is of the form:

$$\int_{-\infty}^{\infty} dk_z \frac{M_n(k_\rho, \pm k_z, r)M_{-n}(-k_\rho, \mp k_z, r')}{(k^2 - k_0^2)k_\rho^2} \tag{9}$$

Since the numerator of the above integrand has no k_z dependence i.e. (goes as a constant), the whole integrand vanishes on a large semi-circle in both the upper and lower k_z half-plane, which enables us to use the residue theorem. The fact that we can close the integration contour in both half-planes is due to the denominator being quadratic in k_z and that the choice of the half-plane dictates the orientation of the contour. Therefore, the k_z integral is independent of the choice of integration contour. We choose to close the contour in the lower half-plane, thereby picking up the $k_{0z} = \sqrt{k_0^2 - k_\rho^2}$ pole contribution, and we have

$$-\frac{\pi j}{\sqrt{k_0^2-k_\rho^2}} M_n(k_\rho, \pm k_{0z}, r) M_{-n}(-k_\rho, \mp k_{0z}, r') \tag{10}$$

The TE_z dyadic can be integrated analogously.

As an example, we give here the expression for the $\hat{\rho}\hat{\rho}$ dyad integral is, being of the form

$$\int_{-\infty}^{\infty} dk_z \frac{1}{(k^2-k_0^2)k_\rho^2} \frac{k_z^2 k_\rho^2}{k^2} J_n'(k_\rho \rho) J_{-n}'(k_\rho \rho') e^{-jn(\phi-\phi')}, \tag{11}$$

and having poles at $k_z = \sqrt{k_0^2 - k_\rho^2}$ and $k_z = -jk_\rho$ (since we keep in accord with the convention to close the contour in the lower half-plane). (13) is then reduced to the sum of the residues

$$\begin{aligned} -2\pi j \Bigg(& \lim_{k_z \to \sqrt{k_0^2-k_\rho^2}} \left(k_z - \sqrt{k_0^2-k_\rho^2}\right) \frac{J_n'(k_\rho \rho) J_{-n}'(k_\rho \rho') k_z^2}{\left(k_z - \sqrt{k_0^2-k_\rho^2}\right)\left(k_z - \sqrt{k_0^2-k_\rho^2}\right)(k_z^2+k_\rho^2)} \\ & + \lim_{k_z \to -jk_\rho} (k_z + jk_\rho) \frac{J_n'(k_\rho \rho) J_{-n}'(k_\rho \rho') k_z^2}{(k_z - jk_\rho)(k_z + jk_\rho)\left(k_z^2 - (k_0^2 - k_\rho^2)\right)} \Bigg) e^{-jn(\phi-\phi')} \\ & = \frac{\pi}{k_0^2}\left(-j\sqrt{k_0^2-k_\rho^2} + k_\rho\right) J_n'(k_\rho \rho) J_{-n}'(k_\rho \rho') e^{-jn(\phi-\phi')} \end{aligned} \tag{12}$$

Suitable extractions from (12) have been performed to isolate its no-converging part (they give rise to delta function terms) and to regularize the integral, which can be performed numerically with suitable numerical quadrature formulas. The same approach has been performed on all the components of the dyadic, resulting in a representation dealing with converging integrals, easy to evaluate, and fully-dyadic singularities expressed in explicit forms.

II – Numerical Results

In this section, some results are shown of analyses performed with the full-wave code implementing the Green's functions briefly described in the previous section, in order to validate our approach.

The structure under analysis is a pin-made slotted waveguide antenna **Erreur ! Source du renvoi introuvable.** shown in Fig. 2. The radiating part is composed by eight radiating slots preceded by a phase shifter. A waveguide port is used to feed the structure.

The equivalent magnetic current over each slot have been described using five entire domain basis functions. The MoM scheme implements the Green's functions described in Section I. The effect of posts is taken into account by a numerically synthesized correction in terms of cylindrical waves.

Figures 3 (a) and 3 (b) show a successfully comparison of the radiated far-field with the finite-element commercial code HFSS in the H-plane at the frequencies of 24.15 GHz and 25.15 GHz.

The agreement between the full-wave simulations and the presented method is very good in all

considered cases. The data have been generated using a Personal Computer with a 2.83GHz Intel Xeon E5440 CPU. The computation time required by the presented method was of 71 s, while HFSS converged in 1968 s. The memory used by the method was 70 MB, while HFSS used 1.6 GHz per each frequency sample. These and other results demonstrate that the proposed algorithm is very efficient in terms of both computational and memory requirements.

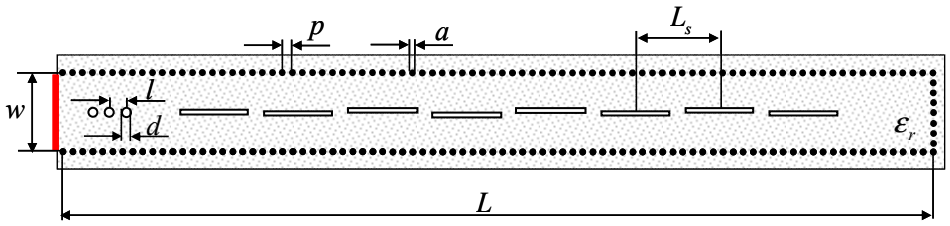

Fig. 2. Slotted SIW antenna. $\varepsilon_r = 2.2$, $h = 0.508$ mm, $L = 66.4$ mm, $W = 5.76$ mm, $p = 0.8$ mm, $a = 4$ mm, $l = 0.8$ mm, $d = 0.4$ mm.

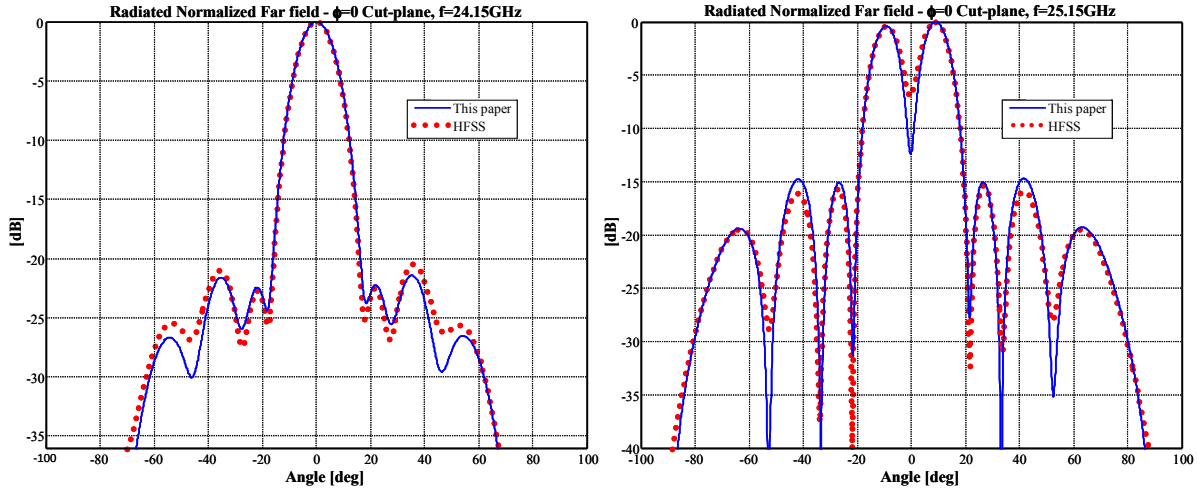

(a) (b)

Fig. 3. Far field radiated by the slotted SIW (Fig. 2) in the H-plane at 24.15 GHz (a) and 25.15 GHz (b).

References

[1] D. Deslandes, and K. Wu, "Integrated microstrip and rectangular waveguide in planar form," *IEEE Microwave and Wireless Components Letters*, vol.11, no.2, pp.68-70, Feb 2001.

[2] M. Bozzi, L. Perregrini, K. Wu, P. Arcioni "Current and Future Research Trends in Substrate Integrated Waveguide Technology," RadioEngineering, vol.18, no.2,pp.201-209, June 2009.

[3] Cuilin Zhong; Jun Xu; Zhiyuan Yu; Yong Zhu; , "Ka-Band Substrate Integrated Waveguide Gunn Oscillator," *IEEE Microwave and Wireless Components Letters*, vol.18, no.7, pp.461-463, July 2008.

[4] W.-K. J. Hirokawa and M. Ando, "Single-layer feed waveguide consisting of posts for plane TEM wave excitation in parallel plates," *IEEE Transactions on Antennas and Propagation*, vol. AP-46, pp. 625–630, May 1998.

[5] Sehyun Park; Okajima, Y.; Hirokawa, J.; Ando, M. , "A slotted postwall waveguide array with interdigital structure for 45° linear and dual polarization, " *IEEE Transactions on Antennas and Propagation,* vol.53, no.9, pp. 2865-2871, Sept. 2005

[6] M. Ettorre and R. Sauleau, “Antenne multicouche à plans parallèles de type pillbox et système d’antennes correspondants,” France Patent FR0952158, Apr. 2009.
[7] M. Ettorre, R. Sauleau, and L. Le Coq, “Multi-beam multi-layer leakywave SIW pillbox antenna for millimeter-wave applications,” *IEEE Trans. Antennas Propag.*, vol. 59, no. 4, pp. 1093-1100, Apr. 2011.
[8] M. Ettorre, A. Neto, G. Gerini, S. Maci, “ Leaky-Wave Slot Array Antenna Fed by a Dual Reflector System”, IEEE Transactions on Antennas and Propagation, Vol. 56, no.10, pp. 3143-3149, Oct. 2008.
[9] M. Ettorre, E. Gandini, and R. Sauleau “Mechanical Scanning with a Dual-Layer Pillbox Antenna for Millimeter-Wave Applications,” *European Conference on Antenna an Propagation EuCAP-2011*, April 11-15, Rome, Italy.